

# EFFECT OF POST-PROCESSING ON THE MICROSTRUCTURE AND MECHANICAL PROPERTIES OF ULTRA-LOW CARBON STEEL FABRICATED BY SELECTIVE LASER MELTING

B. Almangour, J. M. Yang

Department of Materials Science and Engineering, University of California Los Angeles, Los Angeles, CA 90095, USA

REVIEWED

## Abstract

In this study, the effects of heat treatments and hot-isotactic pressing (HIP) on the microstructure and mechanical properties of ultra-low carbon steel produced using selective laser melting (SLM) were investigated. Powder and prototypes characterizations including XRD phase analysis, microstructural observations, and hardness were performed. It was found that heat treatments at 1000 °C and HIP process improved inter-particle bonding very slightly. Significant increases in the grain size were observed for the annealed specimens at 600°C and above as well as after HIP due to recrystallization and further grain growth, which coincide with the drop in hardness.

**Keywords:** Additive manufacturing; selective laser melting; porosity; heat treatment; HIP

## Introduction

Additive Manufacturing (AM) is a group of advanced technologies used to fabricate engineering prototypes of parts through layers material addition based on a digital 3D design data of the item. [1]. The starting material feedstock are shaped and consolidated to build up an arbitrary configuration, given that a computer model of the part has been generated on a computer-aided design (CAD) system [2]. The current trend exhibited in the field of AM is producing of complex and flexible functional components so that they may meet the demands, standards and qualities required by several applications including automotive, aerospace, biomedicine, and the defense [3]. The unique advantage of AM is the possibility to build geometries that are very difficult to fabricate using traditional manufacturing techniques due to its additive approach; i.e. design freedom [4, 5]. This makes it less costly to print because it can be made faster. It is also more flexible because it can be changed in any format in reference to the original CAD file [3, 4]. AM depends on market demand to produce components that are relatively fully dense with mechanical properties like those of the bulk materials [6]. Selective Laser Melting (SLM), in which it is part of AM technologies, powders are heated to just below their melting point to facilitate bonding and reduce distortion of the finished product [7, 8]. One characteristic with SLM is the refinement of the microstructure through increasing the rate of cooling rate, and increases oxidation through restricting removal of oxygen [9-11], which results in higher strengthening.

Numerous scientific researches with SLM of iron-based alloys show several challenges. The finishing of the SLM of iron-based materials is said to be rough [12]. Indeed, there is no uniform distribution of its particles and components causing a weak bonding within the matrix [13]. In general, the densification rate of the SLM of iron parts increased as the density of the applied laser energy increased. However, increased reaction temperature (because of higher laser

power) and the inert atmosphere culminate to decomposition of  $\text{Fe}_2\text{O}_3$  into  $\text{FeO}$  and  $\text{Fe}$  and oxygen that escapes from the specimen [6]. On this basis, higher laser power (causing higher temperatures/heating) contributes to removal of oxygen through intensifying the melting, decomposition, and evaporation. During the processing of SLM of steel, the microstructure suffers from several defects mainly porosity and shrinkage, which are very undesirable solidification defects [7, 14-18]. Besides, the loss of ductility and development of residual stresses may not be desirable for many applications.

Post-processing treatments offer significant improvement to the density of the objects and hence to the mechanical properties. It improves distribution and particles consolidation resulting in a strong particle-particle bonding [11, 19-21]. Heat treatments and Hot-Isotactic Pressing (HIP) therefore could help in eliminating some of the side effects of SLM, discussed above. It is an attempt to increase the strength and ductility by properly varying their microstructure. Limited attention has been made on studying the influence of heat treatments and HIP on the microstructure and mechanical properties of SLM materials. Therefore, in this study, the effect of annealing at different temperatures as well as HIP treatment on the microstructure, phase distribution, and the mechanical properties using compression tests and hardness tests are investigated; for the purpose of comparison a conventional sample are tested using the same characterization tools.

### **Experimental procedures**

#### **Feedstock powder, and SLM processes**

The starting powder is low carbon steel powder (Hoeganes Company), which displays a general irregular shape (Fig. 1a). The composition of the feedstock is an iron matrix with 0.07 wt. % C (Table 1). The sizes of grains in powder particles were around  $2\mu\text{m}$ , observed from the single etched particle (Fig. 1b). From the ground and polished particles, we can confirm that the particles are almost dense (Fig. 1c). The particle size distribution of the powder shows a mean value of about  $20\mu\text{m}$  (Fig. 2).

Processing of samples by SLM was carried out using an SLM 250 HL machine (SLM solutions) equipped with an Yb-YAG laser. The working chamber provides a closed environment filled with an argon-gas in order to prevent the oxidation of steel during the fabrication process. A steel plate was used as the building platform. Before being installed, this platform was grit-blasted with alumina. Using several trials, small steel cubes measuring  $5\text{mm} \times 5\text{mm} \times 5\text{mm}$  dimensions were finally fabricated using the processing parameters shown in Table 2.

#### **Heat treatments and hot-isotactic pressing (HIP) process**

Isothermal heat treatments of 1 h were performed in air using an electric resistance furnace and subsequently air cooled. The numbers of investigated heat treatment temperatures are: 400, 800, 600, and 1000 °C for microstructure and mechanical properties characterizations. The HIP processing takes place at 1162 °C with a  $\pm 3$  °C tolerance. The operating pressure is 14,750 Psi with a  $\pm 250$  Psi tolerance while the treatment time is 3 hrs  $\pm 15$  minutes.

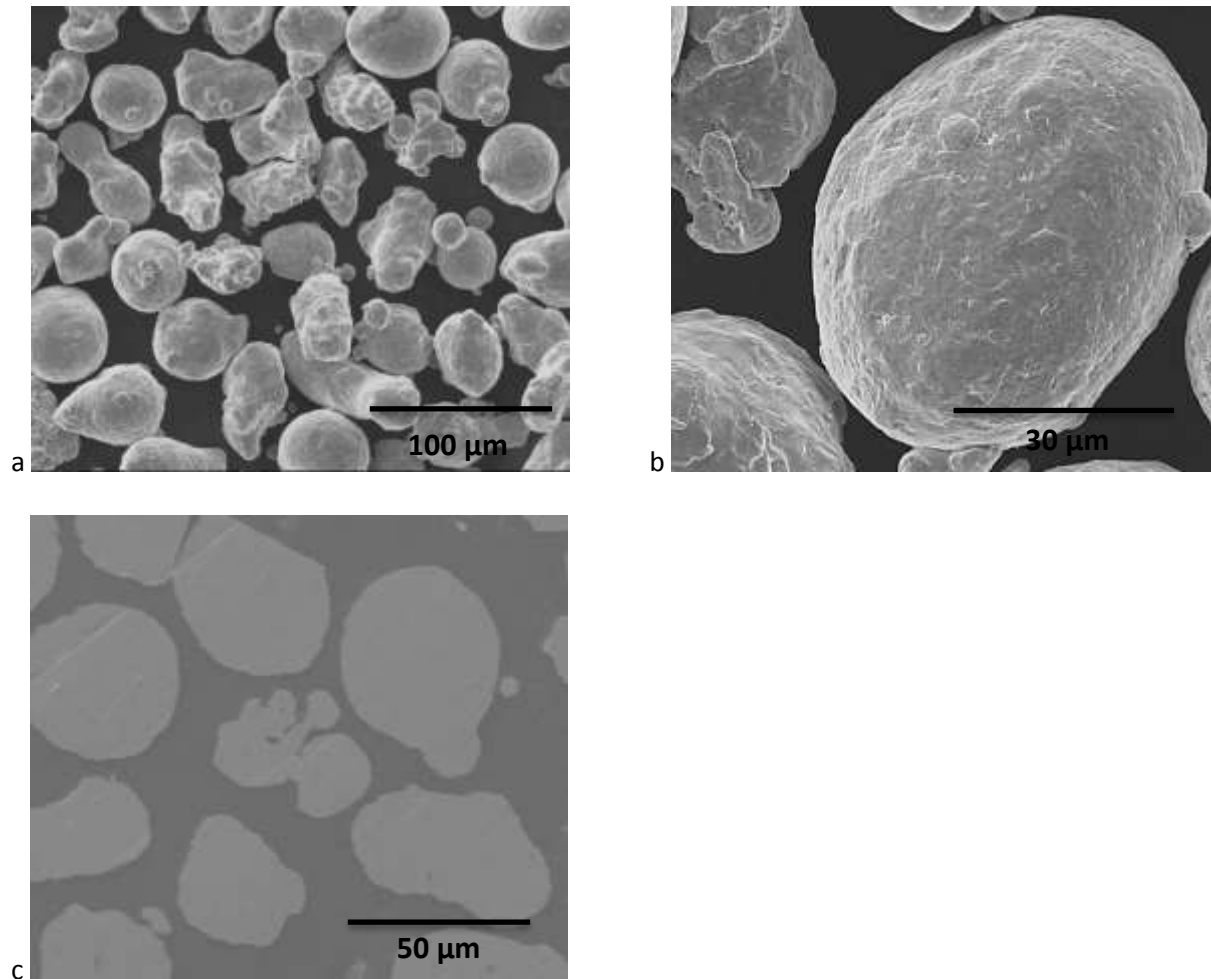


**Figure 1:** (a) SEM micrograph of ultra-low carbon steel powder; (b) single etched particle; (c) polished particles.

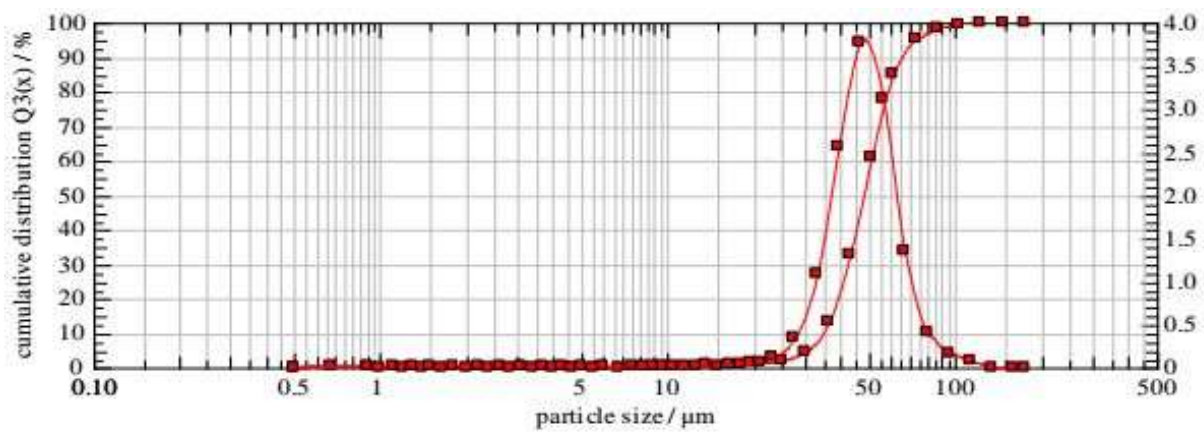


**Figure 2:** ultra-low carbon steel particle size distribution

**Table 1:** Ultra-low carbon steel composition

C	Mn	O	S	Si	Cr	Ni	Fe
0.07 max	0.04 max	0.26 max	0.009 max	0.06 max	0.09	0.01	Balance

**Table 2:** SLM processing parameters

Power for area volume	Atmosphere	Scanning speed for area volume	Layer thickness
175 W	Argon	688 mm/sec	30 $\mu$ m

### Microstructural characterizations

Samples were mechanically grounded and polished with progressively finer grit papers using the standard metallographic techniques and etched in 3% Nital reagent. The surface and the cross-sectional microstructures of the steel cubes were observed using a Nova 230 Nano scanning electron microscope to characterize the powder and fabricated samples. XRD measurements were conducted on a Bruker- binary V1 instrument, operating with a cobalt anticathode at 35kV and 40 mA; the scan step time is 25.6 min in the angular range ( $2\theta$ ) 30-90°.

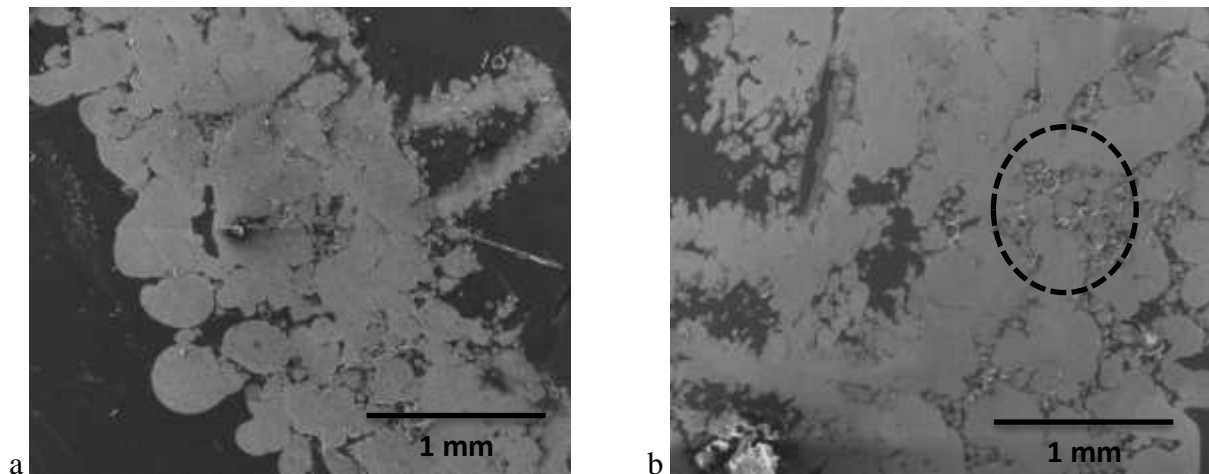
### Mechanical testing

Vickers indentations was performed (Leco, LM800AT) at a small load of 10 g at 15 random particle locations. The hardness of the as-built, annealed, and HIP samples were also measured using a Vickers microhardness tester at a load of 100g for a minimum of 15 measurements taken at random locations on the polished surface. Nano hardness on the polished powder, as well as as-built, annealed, and aged samples were also performed using an MTS nano indentation tester at room temperature.

## Results

### Microstructural characterizations

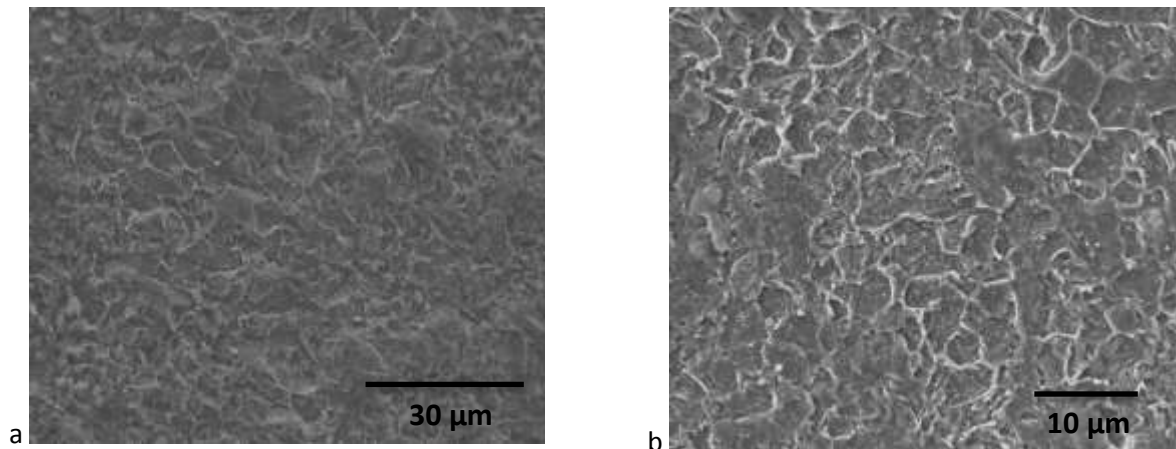
Figure 3a shows the microstructure of the as-built sample, showing some cracking, which suggest that high thermal stresses and thermal deformation were induced during the process. This means that the thermal stresses created during the high heat energy input resulting from low scan speeds have more effect than the C-content on inducing cracks. Besides, carbon may results in some brittleness (0.07% compared relatively to 0.03% found in the 316L stainless steel). In general, the energy available for consolidation is considered to be reduced by two effects. First, partial reflection from the previously scanned line, and secondly, the need to remelt previously proceed material. Only minor porosity was removed after implementation of HIP as shown in Fig. 3b (see dashed circle). HIP was performed at high temperature but still below the melting point, so there is no liquid phase formed during the HIP process. Also, HIP was performed under isotactic pressure, so there is a minimal effect of gravity in aiding the densification by flow of liquid in the direction of gravity (i.e. the thickness or build direction).



**Figure 3:** Cross-sectional microstructure of ultra-low carbon steel: (a) as-built; (b) after HIP.

The etched microstructures of as-built and after HIP treatment from top and side views are shown in Fig. 4. The as-built sample shows very fine grain size as a result of fast cooling. It was seen that grains are of different sizes, may be due the varying thermal heat fluxes during every scanning tracks. After HIP, uniform coarse equiaxed grains were developed and annealing twins throughout the structure (Fig. 4c, Fig. 4d).

At lower heat treatment temperatures of 400 °C and 600 °C, the structure remain unchanged relative to the as-built sample in Fig. 5b. A relatively uniform microstructure of equiaxed grains suggested that recrystallization was complete at 800 °C with further grain coarsening obtained after annealing at 1000 °C (Fig. 5d).



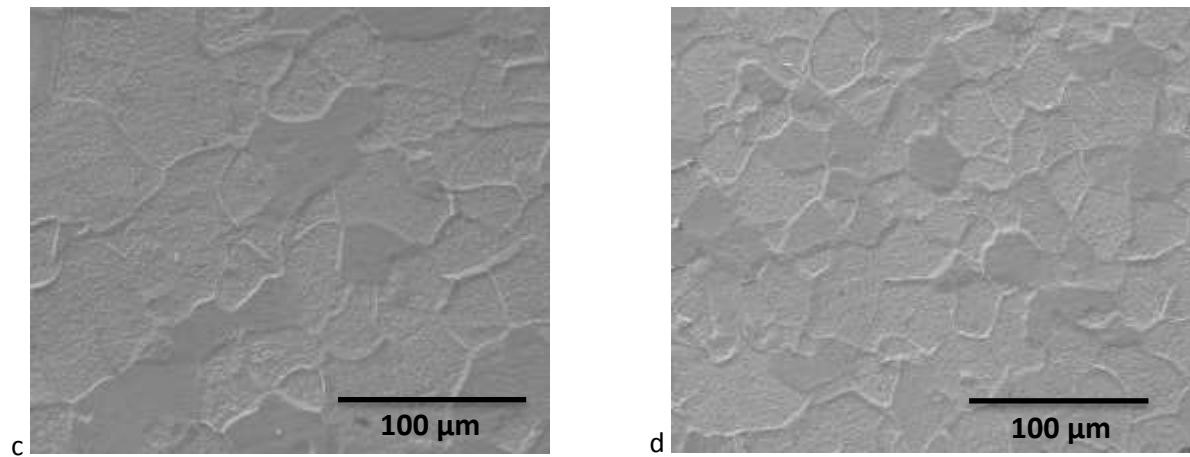


**Figure 4:** Etched cross-sectional microstructure of ultra-low carbon steel: (a) as-built (top view); (b) as-built (side view); (c) after HIP (top side); (d) after HIP (side view).

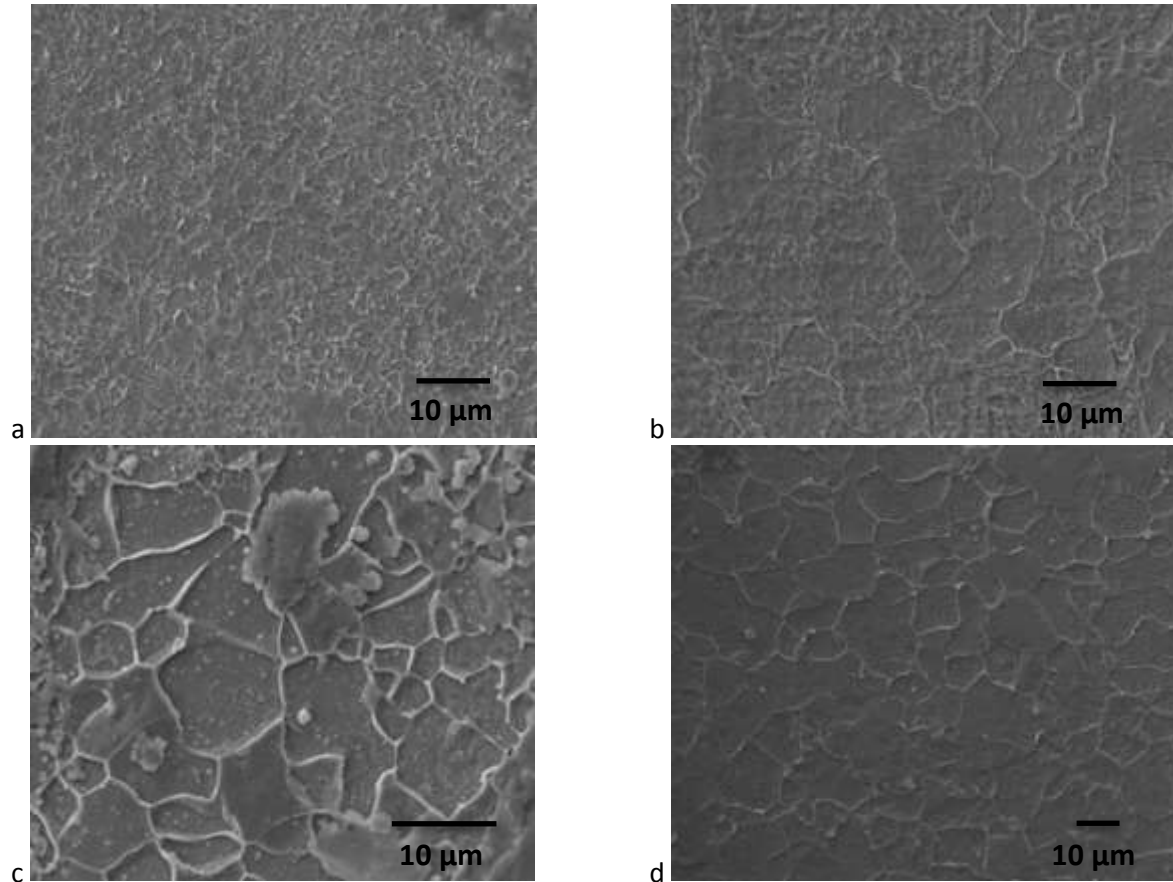


**Figure 5:** Etched cross-sectional microstructure of ultra-low carbon steel: (a) heat treated 400 °C; (b) heat treated 600 °C; (c) heat treated 800 °C; and (d) heat treated 1000 °C.

For comparison purposes, it is clearly shown that the cast sample in Fig. 6b displayed very coarse grains with a mean grain size of 100 $\mu\text{m}$  compared with the as-built sample with a mean grain size of 3 $\mu\text{m}$ . This is attributed to the fast cooling in the SLM process as indicated earlier.

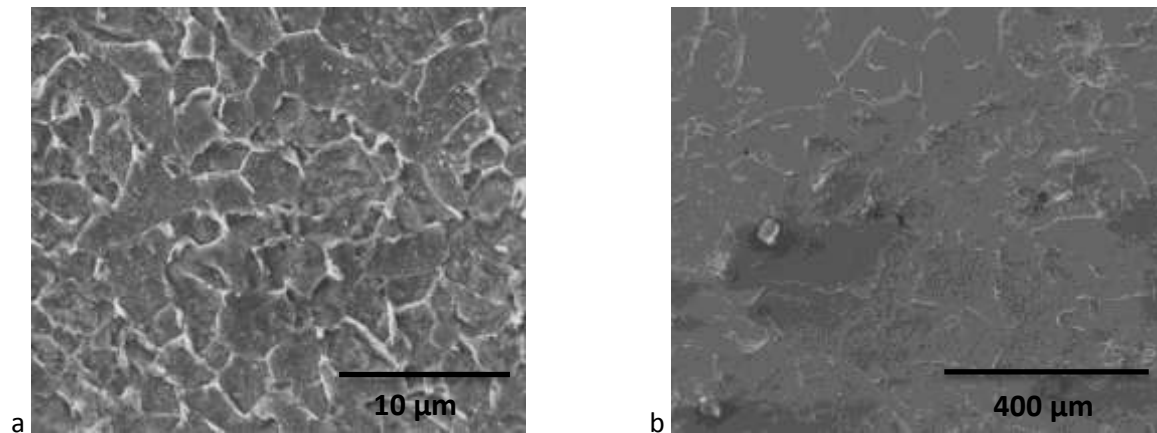


**Figure 6:** Etched cross-sectional microstructure of ultra-low carbon steel: (a) as-built fabricated by SLM; (b) as-cast (conventional).

### XRD analysis

Figure 7 shows the typical XRD histogram for the powder, as-built, and after HIP treatments. It can be seen that the characteristic BCC iron ( $\alpha$  phase) crystalline structure peaks are present in the powder. The XRD pattern of the as-built samples exhibits a significant peak broadening due to the grain refinements as a result of fast cooling. In addition, same set of peaks are displayed in the XRD pattern of the as-built sample indicates that there was no phase transformation or oxidation during fabrication. From the XRD results, no peaks responsible for the carbides can be found in the powder or after fabrication of cubes. There are two reasons why the XRD could not detect carbides. First, the carbon contents are very low and the amount of carbides formed is low. Secondly, due to the quick solidification nature of the SLM process, the dendrites and cells are small and the sizes of the black spots are extremely small. As such, carbide peaks may be too weak to be detected compared to the inherent background noises from the XRD. The XRD profiles after HIP treatment shows typical polycrystalline structure.

Figure 8 shows the XRD pattern for the cube samples after heat treatments. Annealing at 400 $^{\circ}\text{C}$  or 600 $^{\circ}\text{C}$  is similar to the as-built with a slight increase in grain size based on “Williamson-Hall” analysis. However, from annealing of 800 $^{\circ}\text{C}$  and 1000 $^{\circ}\text{C}$ , additional peaks were observed.

It can be seen that the bases of the peaks in the SLM parts are relatively wider than the powder and cast sample (Fig. 9). This suggests that the crystal lattice structures of SLM parts are experiencing certain level of internal stresses that are thermally induced during the rapid solidification of SLM process as discussed earlier. There is also shift of the peaks between the cast and SLM sample to lower angles suggesting the presence of tensile stresses.

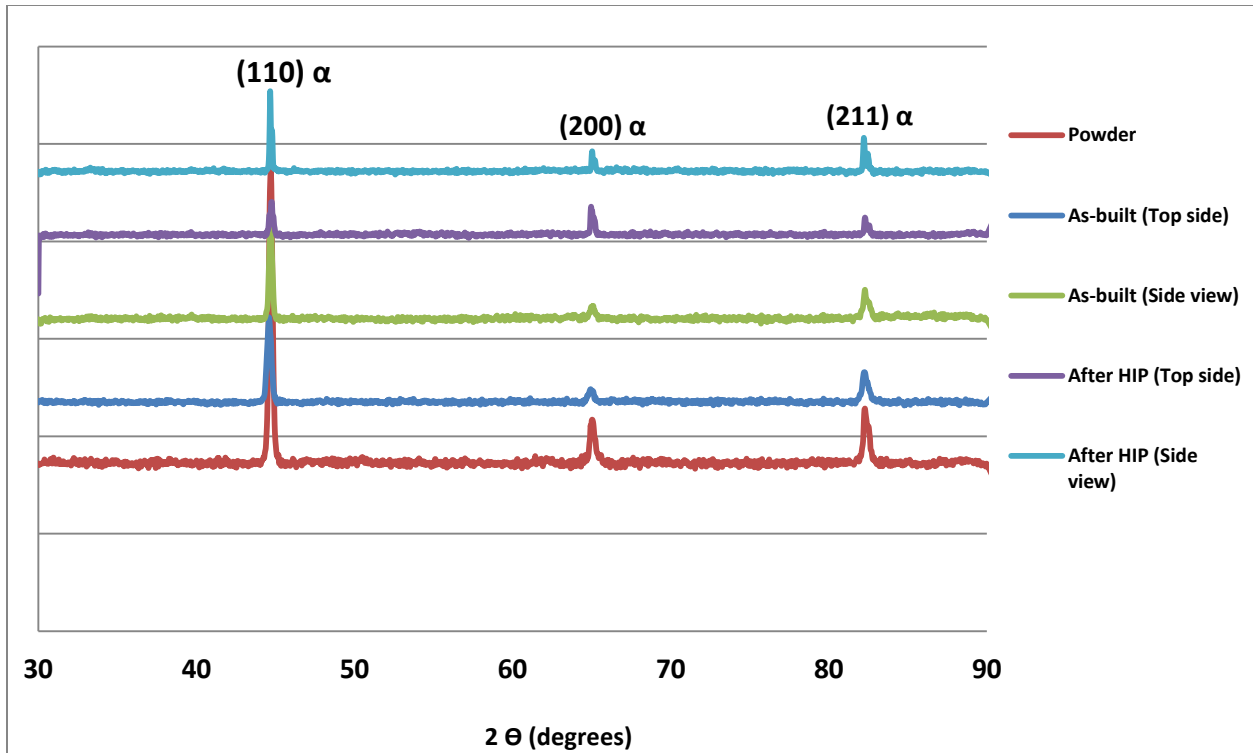


Figure 7: XRD histogram for the powder, as-built, and after HIP treatments.

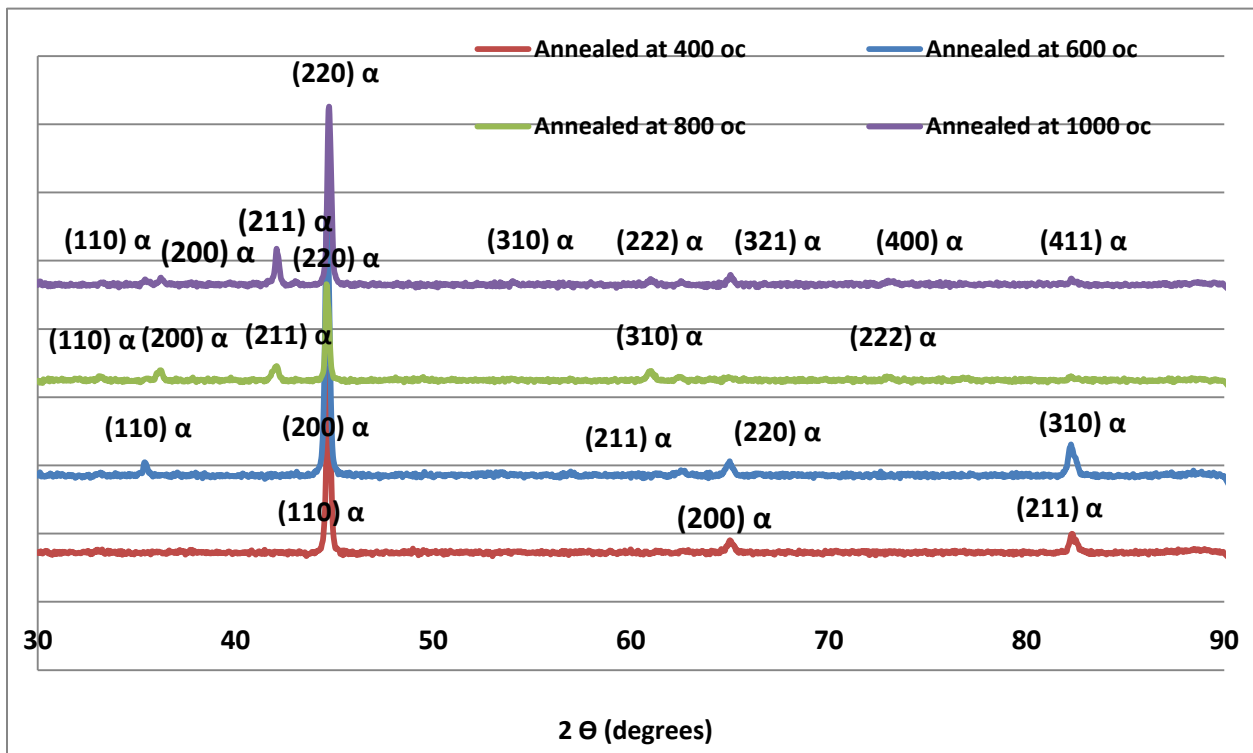
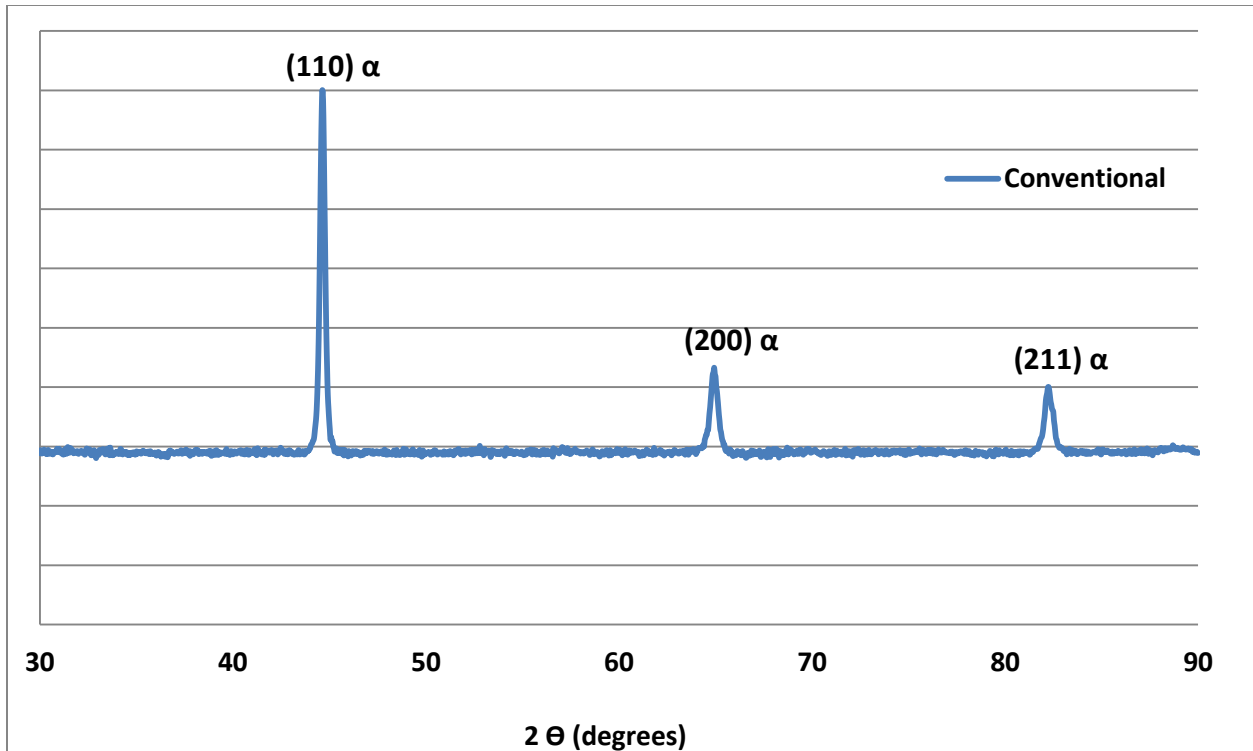


Figure 8: XRD histogram after heat-treatment.



**Figure 9:** XRD histogram of the conventional sample (i.e. casting).

### Mechanical behavior

Figure 10, 11 demonstrates the effect of heat treatment temperatures and HIP treatments of the ultra-low carbon steel on microhardness and nanohardness respectively. The hardness of the as-built increased compared to those of the feedstock powders due to the powder melting followed by rapid solidification. Both scale hardness show stable hardness up to 600 °C, but the hardness drops significantly after annealing at 800 °C; it reduced even further after annealing at 1000 °C as a result of grain growth. After the HIP treatments, the microhardness shows significant drop and similar value for both top and side views because of the homogenization.

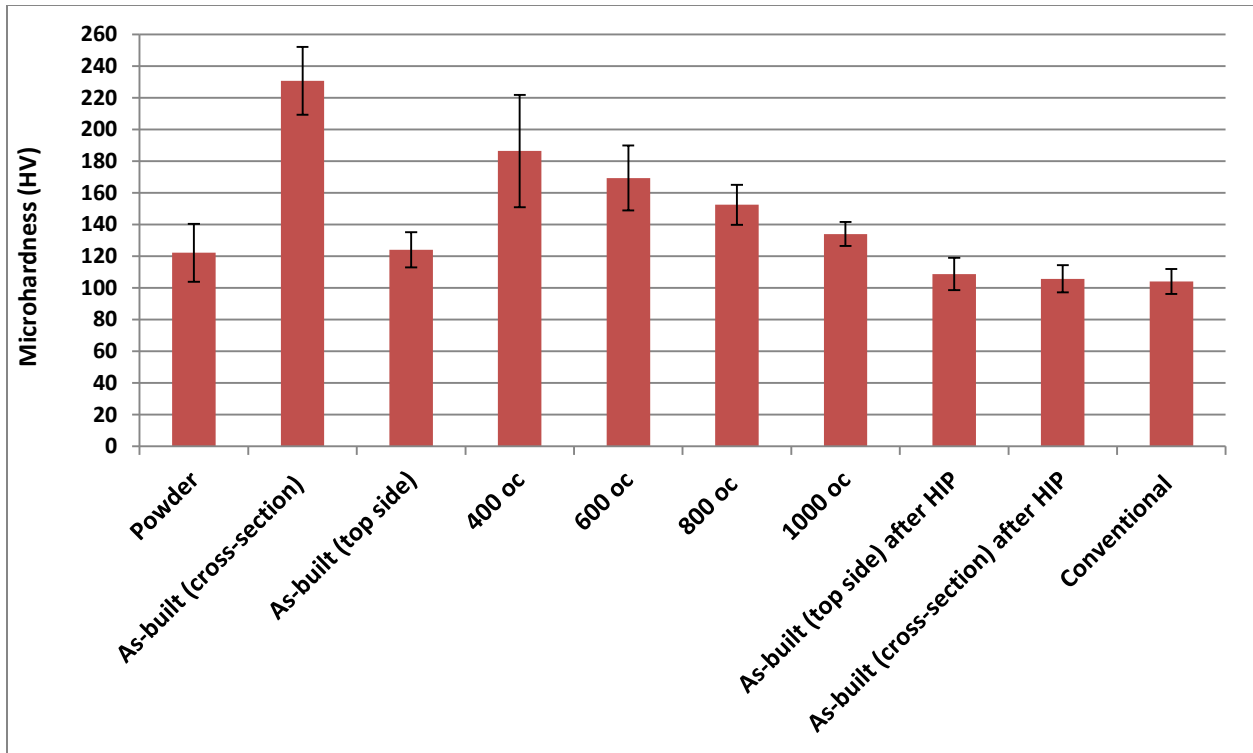


**Figure 10:** Variation of microhardness as a function of heat treatment temperature and HIP treatment.

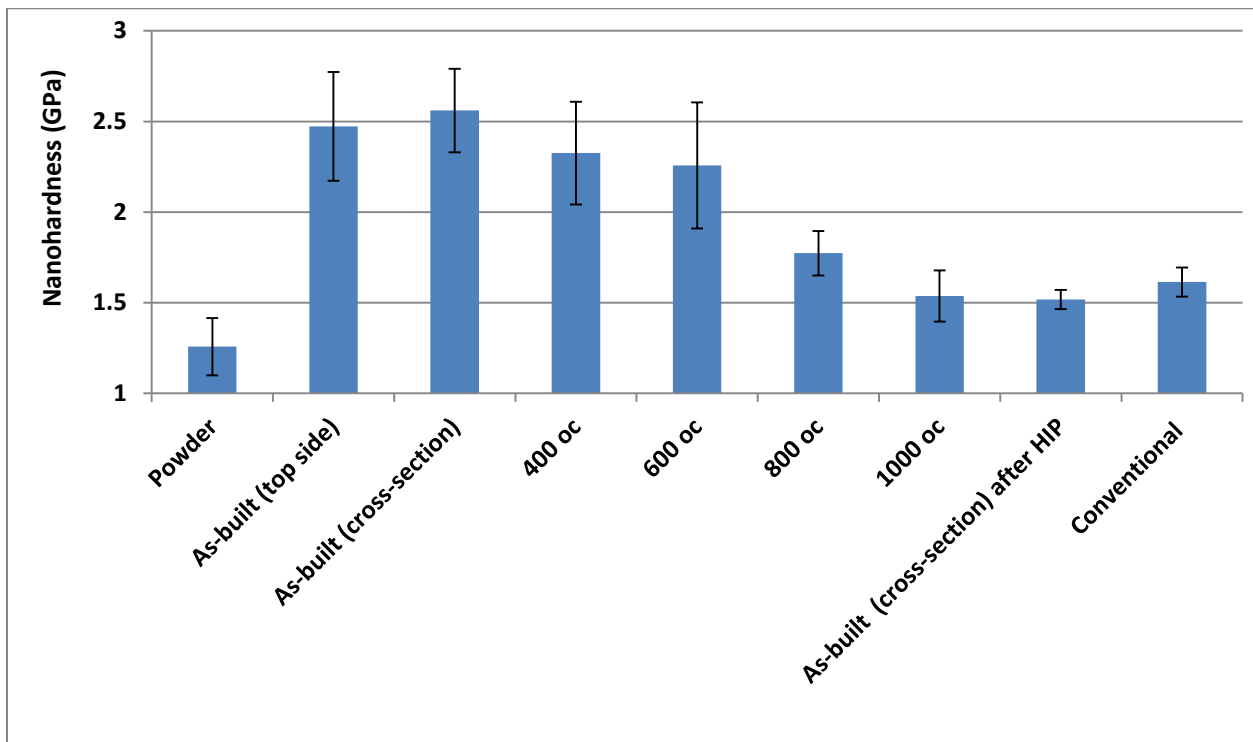


**Figure 11:** Variation of nanoindentation as a function of heat treatment temperature and HIP treatment.

## Discussion

It was deduced, from various research literature, that there was a great challenge of producing carbon steel samples fabricated by SLM, with full density. The difficulty is the result of the special chemical properties of crucial elements within the steel composition. Iron, which serves as a matrix element of steel, is very reactive to oxygen. Therefore, a certain degree of oxidation is unavoidable under normal SLM conditions and powder handling [22]. More so, during laser processing, there is a strong likelihood of occurrence of the “balling phenomena”. This is the result of contamination layer of oxide present on the surfaces of steel melt. Although the carbon content in this study is very low, it is imperative to note that the carbon content of steel plays a critical role in determining processability of SLM. High carbon content also has adverse effect on SLM produced steel, since they portray a limited densification response. Wright et al. [23], found out that with increase in carbon contents, there is an increase in the thickness of the carbon layer accumulated on the melt surface. Just like the oxide layer, the carbon layer has a critical influence mostly on diminishing wettability and causing the melt to spheroidise rather than flow across the underlying surface. In addition to this, the brittleness of SLM manufactured high carbon content steel is increased by the formation of complex interfacial carbides at grain boundaries [24]. Childs et al. [25] through their research, concluded that the dissolution of carbides is favored by increasing the heat flow in the treated powder. On the same breath, increasing heat flow homogenizes distribution of alloying elements. Thus, a thin powder layer thickness, which is less than 100mm, is more recommendable for laser melting. This is besides the optimization of laser types and parameters. Due to this reason, high volumetric energy density for both elemental homogeneity and powder consolidation is achieved [26-28].

During the laser melting process, the metal powder absorbs the laser energy, raises its temperature, melt, and then solidifies when laser moves away, the whole process is less than one second. The heat also transfers away from the melt zone quickly. This causes the melt to cool down rapidly leading to short arrangement time and consequently porosity. In addition, because of the high cooling rate, the gas adsorbed on the surface of the powder, as well generated because of the reaction during the laser melting, have no time to escape from the molten pool and hence porosity was formed.

When free interfaces exist in the system (e.g. liquid-liquid, liquid-gas interfaces) the temperature and compositional gradient will impose a surface tension gradient along the interface, which exerts a shear stress on the fluid. This induces a flow toward regions with higher values of  $\gamma$  termed Marangoni convection [14]. It is observed that during scanning “balling” has occurred. This is caused by surface tension driven by Marangoni convection (i.e. melting instability). Because of the strongly concentrated energy source, a large temperature gradient is often induced on the surface. If the surface tension  $\gamma$  depends on temperature, then the temperature gradient induces a surface flow that can have a considerable influence on the melting pattern. If the surface tension increases with temperature ( $d\gamma/dT > 0$ ), the liquid moves toward the energy beam on the surface, inducing narrower and deeper pool. However, if the surface tension decreases with temperature ( $d\gamma/dT < 0$ ), the surface flow moves away from the energy beam, leading to a wider and shallower pool.

## **Conclusions**

Ultra-low carbon steel powder has been successfully used in the SLM process, and the effects of heat treatments and hot-isotactic pressing (HIP) on the microstructure and mechanical properties were studied. Only minor porosity was eliminated after implementation of HIP and heat treatment at 1000 °C. The SLM processed parts show a uniform fine equiaxed microstructure. The grain microstructure of SLM-fabricated specimens was much finer than that of the cast steel sample due to the high cooling rates associated with the AM process. SEM micrograph revealed that annealing at a temperature 1000 °C and after HIP treatment produced a uniform, fully recrystallized microstructure but with grains much finer than the cast material. It was reported that no difference in the peak patterns until annealing at 800 °C. Further optimizations of the processing parameters are necessary for future work.

## **Acknowledgment**

The authors acknowledge Dr. K. G. Prashanth at Leibniz Institute for Solid State and Materials Research Dresden (IFW) for producing SLM samples. Also, Mr. Brandon Creason at kittyhawkinc is highly thankful for performing the HIP treatments. One of the authors, Bandar AlMangour, would like to extend his appreciation to the Saudi Basic Industries Corporation, which generously awarded financial support to him.

## **References**

- [1] Wong KV, Hernandez A. A review of additive manufacturing. *ISRN Mechanical Engineering* 2012;2012.
- [2] Gu D, Meiners W, Wissenbach K, Poprawe R. Laser additive manufacturing of metallic components: materials, processes and mechanisms. *International materials reviews* 2012;57:133-64.
- [3] Kruth J-P, Leu M, Nakagawa T. Progress in additive manufacturing and rapid prototyping. *CIRP Annals-Manufacturing Technology* 1998;47:525-40.
- [4] Gibson I, Rosen DW, Stucker B. *Additive manufacturing technologies*: Springer; 2010.
- [5] Sercombe TB, Schaffer GB. Rapid Manufacturing of Aluminum Components. *Science* 2003;301:1225-7.
- [6] Kruth J-P, Levy G, Klocke F, Childs T. Consolidation phenomena in laser and powder-bed based layered manufacturing. *CIRP Annals-Manufacturing Technology* 2007;56:730-59.
- [7] Kruth J-P, Froyen L, Van Vaerenbergh J, Mercelis P, Rombouts M, Lauwers B. Selective laser melting of iron-based powder. *Journal of Materials Processing Technology* 2004;149:616-22.
- [8] Kruth J-P, Mercelis P, Van Vaerenbergh J, Froyen L, Rombouts M. Binding mechanisms in selective laser sintering and selective laser melting. *Rapid prototyping journal* 2005;11:26-36.
- [9] Kobayashi KF. *Laser processing*. Pergamon Materials Series 1999;2:89-118.
- [10] Bourell D, Wohler M, Harlan N, Das S, Beaman J. Powder Densification Maps in Selective Laser Sintering. *Advanced Engineering Materials* 2002;4:663-9.
- [11] Prashanth K, Scudino S, Klauss H, Surreddi KB, Loeber L, Wang Z, et al. Microstructure and mechanical properties of Al-12Si produced by selective laser melting: Effect of heat treatment. *Materials Science and Engineering: A* 2014;590:153-60.

- [12] Rajabi M, Vahidi M, Simchi A, Davami P. Effect of rapid solidification on the microstructure and mechanical properties of hot-pressed Al–20Si–5Fe alloys. *Materials Characterization* 2009;60:1370-81.
- [13] Santos EC, Shiomi M, Osakada K, Laoui T. Rapid manufacturing of metal components by laser forming. *International Journal of Machine Tools and Manufacture* 2006;46:1459-68.
- [14] Davis SH. *Theory of solidification*: Cambridge University Press; 2001.
- [15] Verhaeghe F, Craeghs T, Heulens J, Pandelaers L. A pragmatic model for selective laser melting with evaporation. *Acta Materialia* 2009;57:6006-12.
- [16] Rombouts M, Kruth J-P, Froyen L, Mercelis P. Fundamentals of selective laser melting of alloyed steel powders. *CIRP Annals-Manufacturing Technology* 2006;55:187-92.
- [17] Song B, Dong S, Deng S, Liao H, Coddet C. Microstructure and tensile properties of iron parts fabricated by selective laser melting. *Optics & Laser Technology* 2014;56:451-60.
- [18] Liu Z, Chua C, Leong K, Kempen K, Thijs L, Yasa E, et al. A preliminary investigation on selective laser melting of M2 high speed steel. *Innovative Developments in Virtual and Physical Prototyping: Proceedings of the 5th International Conference on Advanced Research in Virtual and Rapid Prototyping, Leiria, Portugal, 28 September-1 October, 2011*: CRC Press; 2011. p. 339.
- [19] Wauthle R, Vrancken B, Beynaerts B, Jorissen K, Schrooten J, Kruth J-P, et al. Effects of build orientation and heat treatment on the microstructure and mechanical properties of selective laser melted Ti6Al4V lattice structures. *Additive Manufacturing* 2014.
- [20] Ma P, Prashanth KG, Scudino S, Jia Y, Wang H, Zou C, et al. Influence of Annealing on Mechanical Properties of Al-20Si Processed by Selective Laser Melting. *Metals* 2014;4:28-36.
- [21] Song B, Dong S, Liu Q, Liao H, Coddet C. Vacuum heat treatment of iron parts produced by selective laser melting: Microstructure, residual stress and tensile behavior. *Materials & Design* 2014;54:727-33.
- [22] Das S. Physical aspects of process control in selective laser sintering of metals. *Advanced Engineering Materials* 2003;5:701-11.
- [23] Wright CS, Youseffi M, Akhtar S, Childs T, Hauser C, Fox P. Selective laser melting of prealloyed high alloy steel powder beds. *Materials science forum: Trans Tech Publ*; 2006. p. 516-23.
- [24] Childs T, Hauser C, Badrossamay M. Selective laser sintering (melting) of stainless and tool steel powders: experiments and modelling. *Proceedings of the Institution of Mechanical Engineers, Part B: Journal of Engineering Manufacture* 2005;219:339-57.
- [25] Childs T, Hauser C, Badrossamay M. Mapping and modelling single scan track formation in direct metal selective laser melting. *CIRP Annals-Manufacturing Technology* 2004;53:191-4.
- [26] Tsopanos S, Mines R, McKown S, Shen Y, Cantwell W, Brooks W, et al. The influence of processing parameters on the mechanical properties of selectively laser melted stainless steel microlattice structures. *Journal of Manufacturing Science and Engineering* 2010;132:041011.
- [27] Yadroitsev I, Shishkovsky I, Bertrand P, Smurov I. Manufacturing of fine-structured 3D porous filter elements by selective laser melting. *Applied Surface Science* 2009;255:5523-7.
- [28] Gusarov A, Yadroitsev I, Bertrand P, Smurov I. Heat transfer modelling and stability analysis of selective laser melting. *Applied Surface Science* 2007;254:975-9.